Radiation activates HIF-1 to regulate vascular radiosensitivity in tumors: Role of reoxygenation, free radicals, and stress granules

Benjamin J. Moeller,[1] Yiting Cao,[1] Chuan Y. Li,[2] and Mark W. Dewhirst[1,2,*]

[1]Department of Pathology
[2]Department of Radiation Oncology
Duke University Medical Center, Durham, North Carolina 27710
*Correspondence: dewhirst@radonc.duke.edu

Summary

Through a poorly understood mechanism, tumors respond to radiation by secreting cytokines capable of inhibiting apoptosis in endothelial cells, thereby diminishing treatment response by minimizing vascular damage. We reveal here that this pathway is governed by a major angiogenesis regulator, HIF-1. Following radiotherapy, tumor reoxygenation leads to: (1) nuclear accumulation of HIF-1 in response to reactive oxygen, and (2) enhanced translation of HIF-1-regulated transcripts secondary to stress granule depolymerization. The resulting increase in HIF-1-regulated cytokines enhances endothelial cell radioresistance. Inhibiting postradiation HIF-1 activation significantly increases tumor radiosensitivity as a result of enhanced vascular destruction. These data describe novel pathways contributing significantly to our understanding of HIF-1 regulation which may be major determinants of tumor radiosensitivity, potentially having high clinical relevance.

Introduction

It has recently been suggested that the sensitivity of tumor vasculature to radiation is a major determinant of overall response to radiotherapy (RT) (Garcia-Barros et al., 2003). This relationship is attributable to the fact that in addition to directly killing tumor cells, ionizing radiation leads to a secondary cell death by destroying the tumor-feeding vasculature. As tumors are highly reliant on their vessels for survival (Folkman, 2002; Folkman and Shing, 1992), small degrees of vascular destruction may translate into large-scale tumor kill (Denekamp, 1993). Thus, the more radiosensitive a tumor's vasculature, the less radioresistant the tumor (Camphausen and Menard, 2002). Maximizing radiation's effects on tumor endothelium may be a powerful new treatment strategy, and there is currently much interest in exploring how this might be done.

An important step toward understanding how the tumor vasculature responds to radiation came from the work of Gorski et al. (1999), who studied the effects of radiation on expression of a prototypical angiogenic cytokine, vascular endothelial growth factor (VEGF). The authors found that radiation induced tumors to secrete VEGF, and that VEGF served to enhance endothelial cell (EC) radioresistance (Gorski et al., 1999). This discovery suggested that tumors actively protect themselves from secondary radiation damage by promoting EC radioresistance. Based on these data, several groups have investigated the effects of combining antiangiogenic agents with radiation in order to maximize EC radiosensitivity (Geng et al., 2001; Hess et al., 2001; Kozin et al., 2001; Lund et al., 2000). Though this work has met with some success, it may be possible to further enhance the efficacy of this approach. The complexity of the mechanism allowing tumors to increase EC radioresistance may have initially been underestimated; it appears now that numerous factors other than VEGF may be involved. Indeed, it has been demonstrated that inhibiting a diverse array of EC tyrosine kinase receptors is significantly more effective at radiosensitizing tumor vasculature than is VEGF receptor blockade alone (Ning et al., 2002). Achieving EC radiosensitization solely by inhibiting VEGF signaling, then, may be incompletely effective due to redundant protective signals provided by additional cytokines.

Currently, very little is known about how RT induces tumors to protect endothelial cells. VEGF secretion is clearly an important component of the pathway, but additional cytokines must also be involved, as discussed above. Ultimately, achieving optimal EC radiosensitization may require inhibition of all vascu-

SIGNIFICANCE

Approximately half of all US citizens diagnosed with cancer are treated with radiotherapy. Recent discoveries suggest that the sensitivity of a tumor's vasculature to radiation is a major determinant of radiotherapeutic outcome. There is currently great interest in working to enhance tumor vessel radiosensitivity, thereby maximizing secondary radiation-induced tumor death caused by vascular destruction. However, tumors avoid this secondary damage by secreting cytokines that diminish vascular radiation damage. We hypothesize that by understanding how this protective response is activated, we can discover an effective means of inhibiting it. This work takes a major step toward achieving this understanding, and might eventually translate into a significant clinical benefit by allowing optimal sensitization of tumor vasculature to conventional therapeutics including radiation.

lar radioresistance-inducing signals. An effective way to do so may be to block these signals at the source—to disrupt a common pathway regulating the radiation-induced secretion of these cytokines by tumors. We hypothesize that this pathway may depend critically on signal transduction through a factor which regulates multiple angiogenic cytokines. One such regulator fitting this description is hypoxia inducible factor-1 (HIF-1). HIF-1 is a heterodimer composed of a hypoxia-regulated α subunit and an oxygen-independent β subunit. The HIF-1 complex is capable of binding to hypoxia regulatory elements (HREs) in the nucleus, stimulating the expression of more than 40 downstream genes involved in tumor metabolism, growth, and angiogenesis, including VEGF (Semenza, 2002). Recently, it has become apparent that several HIF-1-regulated genes other than VEGF are highly active in angiogenesis, including those coding for eryrthropoietin (EPO) (Jaquet et al., 2002), transforming growth factor-β3 (TGF-β3) (Gold et al., 2000), plasminogen activator inhibitor-1 (PAI-1) (Devy et al., 2002), and transferrin (Carlevaro et al., 1997). Moreover, some HIF-1-regulated factors themselves are capable of activating potent proangiogenic proteins. For instance, it has been demonstrated that VEGF induces cells to release bioactive bFGF, proving that this highly active angiogenic cytokine is indirectly regulated by HIF-1 (Jonca et al., 1997). Highly relevant here, VEGF and bFGF are the sole factors which have been directly shown to increase EC radioresistance (Gorski et al., 1999; Paris et al., 2001). Therefore, it may be that HIF-1 activity has a much greater impact on the postradiation tumor-vessel relationship than does VEGF alone.

Thus, in this work we address the question of whether HIF-1 is involved in regulating the response of tumors to ionizing radiation. We investigate whether clinically relevant courses of RT activate HIF-1 in murine and human tumor models. Additionally, we identify molecular pathways involved which provide mechanistic links between radiation exposure and HIF-1 signaling activation. Finally, studies are carried out to determine whether HIF-1 activation is a crucial step in the RT-induced radioprotection of tumor vasculature. These studies have important implications for trials aimed at combining antiangiogenic agents with radiation and, potentially, various other treatment modalities.

Results

Radiation upregulates HIF-1 levels and activity

We first investigated whether radiation upregulates tumor HIF-1 activity. Tumor cell lines stably transfected with a fluorescent reporter of HIF-1 activity were grown in skinfold window chambers. These cells express GFP under the control of an HRE element, the DNA binding site for HIF-1, thereby allowing serial monitoring of HIF-1 activity levels by following GFP expression (Figure 1A). Intravital fluorescence microscopy was used to record reporter activity in these tumors following irradiation (Figure 1B). During fractionated RT, HIF-1 activity decreased slightly. Approximately 12–24 hr after radiation, HIF-1 activity began to increase steadily over time, peaking 48 hr following treatment. Spatially, HIF-1 activation was noted first at the tumor periphery, and migrated toward the center of the tumor between 24 and 48 hr after treatment. As a positive control, window chamber tumors expressing GFP independent of HIF-1 activity (CMV-GFP) were also irradiated. This control group demonstrated no changes in GFP signal intensity or expression patterns (Figure 1C), indicating that the post-RT HIF-1 reporter observations were specific for changes in HRE signaling activity. Quantification of HIF-1 reporter fluorescence intensity over time revealed that irradiation caused statistically significant ($p < 0.05$), dose-dependent increases in tumor HIF-1 activity when compared to nonirradiated controls (Figure 1D). Again, the CMV-GFP control tumors demonstrated no changes in fluorescence intensity following any dose of radiation studied.

To determine whether the observed reporter activity data were reflective of actual changes in HIF-1 signaling, we next studied radiation's effects on protein levels for both HIF-1α and cytokines expressed under its control. Unexpectedly, irradiation of cultured tumor cells did not cause an increase in nuclear HIF-1 protein levels or HIF-1 reporter activity (Figures 2A and 2B), although it did lead to increased secretion of certain HIF-1-regulated cytokines such as VEGF (data not shown). However, in agreement with the window chamber studies, tissue isolated from irradiated flank tumors had significantly ($p < 0.05$) higher nuclear HIF-1 levels when compared to nonirradiated controls (Figure 2C). Mirroring this result, irradiated flank tumors also demonstrated increased levels of the proangiogenic HIF-1-regulated cytokines VEGF and PAI-1, as well as the indirectly regulated bFGF (Figures 2D–2F). These results argue that radiation causes HIF-1 upregulation in vivo but not in vitro, suggesting that an intact tumor-host interface may be required for this response to occur.

RT-induced HIF-1 activation coincides with reoxygenation

The spatiotemporal pattern of radiation-induced HIF-1 activation, described above, is highly reminiscent of reoxygenation (Bussink et al., 2000; Fenton et al., 1998). Thus, we sought to determine whether we could find direct evidence to connect tumor reoxygenation with HIF-1 activation. First, mice with flank tumors stably transfected with the fluorescent HIF-1 reporter were randomized to receive RT or sham-RT. 48 hr later, these animals were injected intravenously with a perfusion marker (Hoechst 33342), and the tumors were removed for analysis via microscopy of flow cytometry (Figures 3A and 3B). Very little evidence of overlap between perfusion and HRE-GFP expression was found in sham-irradiated tumors (1.9% $\pm$ 0.3% double-positive by FACS). This pattern of discordance was retained in tumors following radiation (2.0% $\pm$ 0.4% double-positive), despite the overall increase in reporter signal intensity. Thus, radiation-induced HIF-1 activation, like physiologic tumor HIF-1 activation, occurs in tumor cells that are distant from perfused vasculature.

Following irradiation, tumor oxygenation tends to increase secondary to various complicated physiological responses (Dewhirst et al., 1990). Although reperfusion may be involved, decreased oxygen consumption by tumor cells allows for oxygenation to improve even in the absence of increased perfusion (Kallman, 1972). In our model, then, irradiated tumor tissue that is distant from perfused vessels (i.e., the GFP^+ tissue described above) may be better oxygenated than it was before RT. To test this hypothesis, we administered a hypoxia marker drug, pimonidazole, 48 hr after irradiating HRE-GFP-reporting tumors. Nonirradiated tumors demonstrated tight colocalization of GFP and pimonidazole signals; irradiated tumors contained a significantly smaller proportion of GFP^+ tissue colocalizing with pimonidazole (Figure 3C). For sham-irradiated tumors, 91.3 $\pm$ 3.3% of the total GFP^+ tumor tissue area was associated with

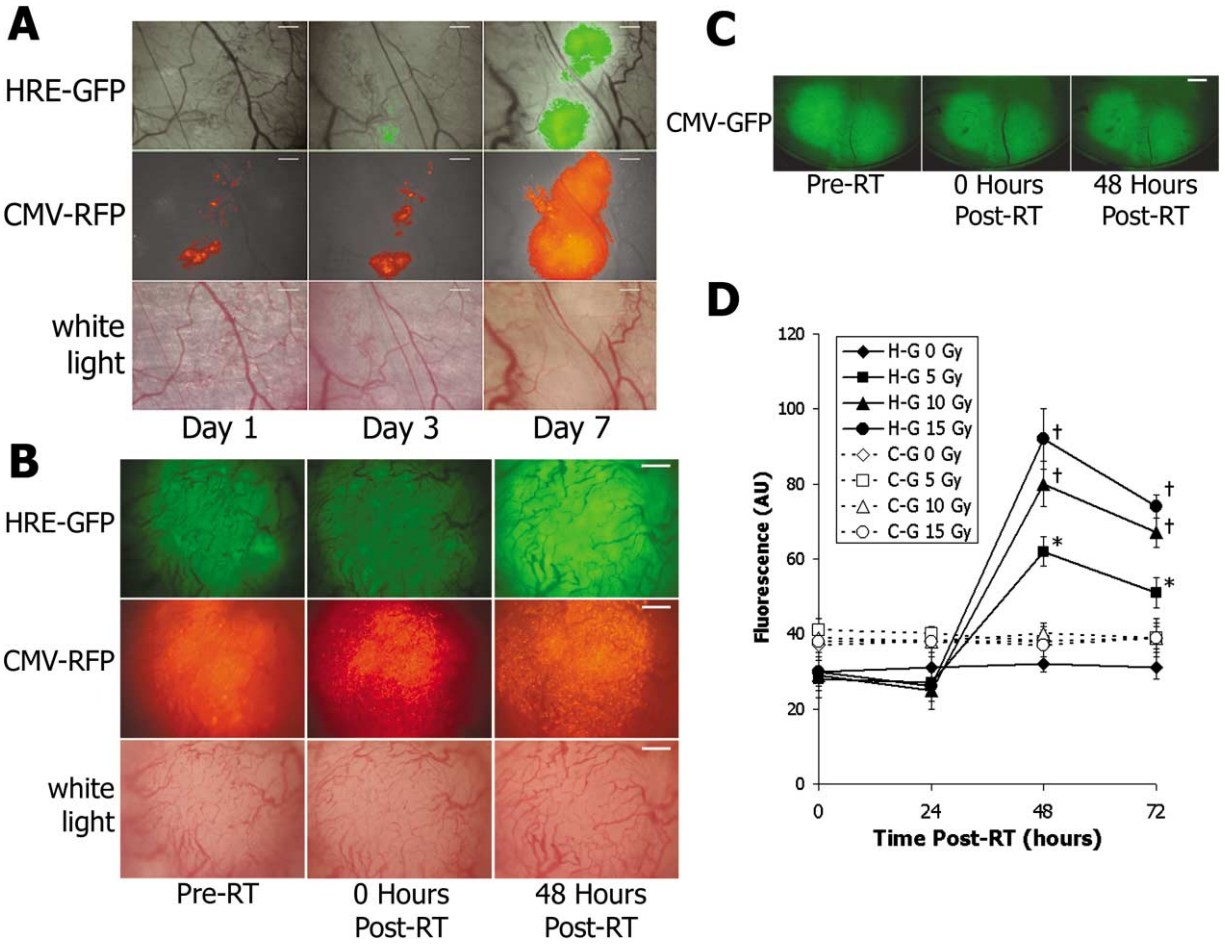

Figure 1. RT induces HIF-1 reporter activation

A: Representative baseline HIF-1 reporter activity in window chamber 4T1 tumors at days 1, 3, and 7 following tumor implantation. Tumors typically became sufficiently large and vascularized for irradiation between days 12 and 14. Bar = 300 μm.
B: Representative post-RT HIF-1 reporter activity in window chamber 4T1 tumors. Following radiation, upregulation began at the tumor periphery, and peaked at 48 hr post-RT. Note that vascular growth proceeds following RT, indicating an apparent radioresistance of the tumor vasculature. Bar = 300 μm.
C: Irradiation of window chamber 4T1 tumors constitutively expressing GFP (CMV-GFP) caused no change in fluorescence intensity.
D: Longitudinal quantification of GFP fluorescence intensity in tumors expressing HIF-1-inducible GFP (H-G) and constitutive GFP (C-G) following irradiation with 0 Gy, 5 Gy, 10 Gy, or 15 Gy. *, $p < 0.05$; †, $p < 0.005$, versus non-irradiated tumors.

pimonidazole, but this association occurred for only 18.0 ± 0.8% of irradiated tumor tissue (Figure 3D). These results indicate that the majority of HRE signaling in irradiated tumors occurs in tissue with relatively high oxygenation levels. This is contrary to the normal paradigm of HIF-1 upregulation by hypoxia, making it a striking finding strongly supporting the conclusion that radiation-induced HIF-1 activation coincides with tumor reoxygenation.

Free radical species link reoxygenation to HIF-1 activation

Having linked radiation-induced tumor reoxygenation with HIF-1 activation, we next sought to understand the mechanisms connecting the two. As has been suggested by in vitro studies (Hammond et al., 2003), reoxygenation of hypoxic tumor cells may induce the formation of free radicals. Moreover, ROS have been shown to be both necessary (Chandel et al., 1998) and sufficient (Chandel et al., 2000) for HIF-1 activation. Therefore, we hypothesized that radiation-induced tumor reoxygenation, in vivo, might generate enough oxidative stress to stabilize HIF-1.

In order to investigate this hypothesis, we developed a novel assay to permit serial in vivo monitoring of tumor free radicals. Skinfold window chamber tumors were suffused with media containing the free radical-sensitive dye carboxy-2′7′-dihydrodichlorofluorescein diacetate (H_2DCFDA), which is converted to the fluorescent DCFDA when exposed to various free radical species. DCFDA, whose fluorescence is not free radical-responsive, was used in a control group of tumors to rule out nonspecific radiation effects on dye accumulation. As a further control, tumors were treated after RT with a small molecular weight mimetic of superoxide dismutase (SOD) with potent catalytic activity against a variety of free radical species (Batinic-Haberle et al., 1998). It was reasoned that if H_2DCFDA incubation revealed an increase in tumor ROS and RNS following RT, it should be possible to reverse this effect with the SOD mimetic.

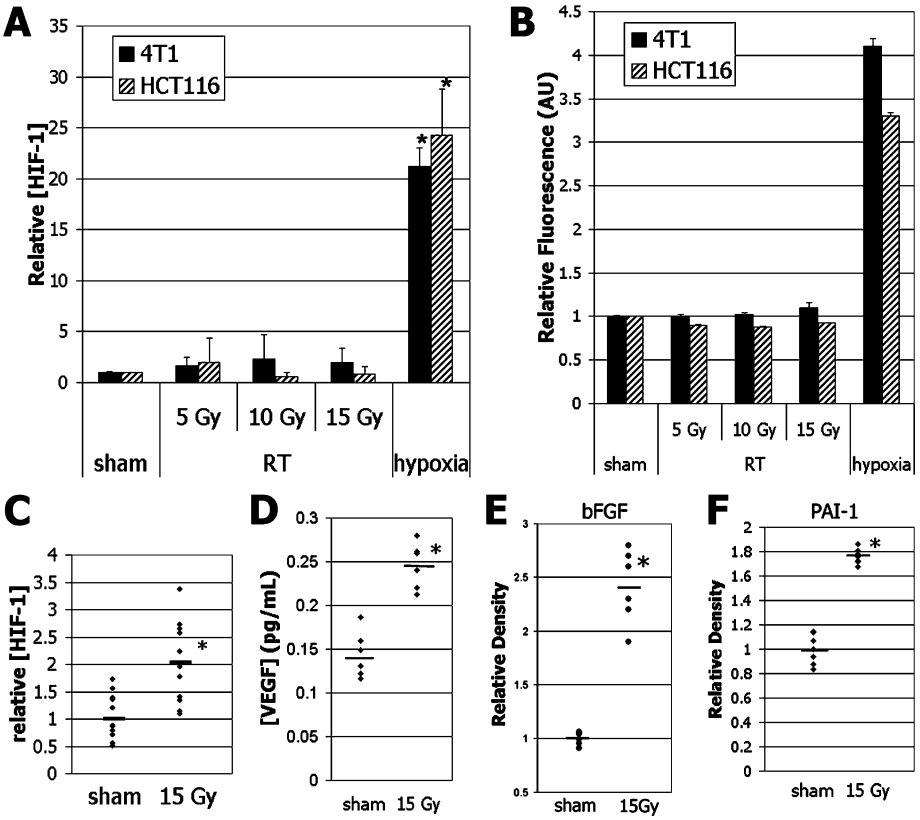

Figure 2. RT induces upregulation of HIF-1 and downstream cytokines

A and B: Irradiation of tumor cell lines in vitro caused no detectable increase in HIF-1 nuclear levels or reporter activation at 48 hr post-RT. Data were essentially identical at 24 and 72 hr post-RT (not shown). Positive controls are shown for comparison. Results were normalized to the mean sham-treated value.

C–F: Quantification of HIF-1, VEGF, FGF, and PAI-1 protein levels in excised flank 4T1 tumors. Actual data points shown; bar represents mean. For HIF-1, FGF, and PAI-1, results were normalized to the sham-treated mean values. *, $p < 0.05$, versus nonirradiated tumors.

Following a short RT course (two 5 Gy fractions), the free radical-sensitive H_2DCFDA signal was seen to increase dramatically over that seen before treatment (Figure 4A), while no changes in the free radical-insensitive DCFDA signal intensity were observed. When the SOD mimetic was administered following completion of RT, the radiation/reoxygenation-induced H_2DCFDA response was completely suppressed (Figure 4A), validating the specificity of the assay. These results confirm, then, that RT leads to a delayed increase in tumor oxidative stress coinciding with reoxygenation.

Next, we studied whether oxidative stress could increase HIF-1 levels in tumors. In agreement with previous reports (Chandel et al., 2000), exposure of cells to 10 μM H_2O_2 for 10 hr caused approximately 2-fold increases in nuclear HIF-1 levels (Figure 4B). This effect was abrogated in the presence of equimolar concentrations of the SOD mimetic. Similarly, reactive nitrogen species generated by the NO donor NOC-18 (DETA-NONOate) caused nuclear accumulation of HIF-1 in cultured tumor cells (Figure 4C). Next, we asked whether scavenging tumor free radicals after RT could also suppress the stimulus for postradiation HIF-1 accumulation in vivo. In both the flank tumor and dorsal skinfold window chamber models, antioxidant treatment delivered after the completion of radiotherapy completely blocked nuclear HIF-1 upregulation and reporter gene activation, respectively (Figures 4D and 4E). Importantly, when HIF-1α was blocked in this way, dramatic destruction of the tumor vasculature was observed, beginning shortly after the time of typical peak radiation-induced HIF-1 activation (Figure 4E).

As antioxidant treatment inhibited radiation/reoxygenation-induced HIF-1 activation, and since the tumor vasculature appeared highly dependent on this response, we next asked whether postradiation free radical scavenging could significantly improve radiotherapeutic tumor control. Flank tumors were randomized to treatment with or without radiation, then with or without SOD mimetic injection. Again, this free radical scavenger was administered after the completion of RT so that interference with the initial ROS induced by ionizing radiation could be avoided. Whereas SOD mimetic administration had little impact on tumor growth, combining it with radiation led to significant enhancement of tumor growth delay (Figure 4F). Together, these results confirm the importance of free radical species, stimulated during radiation-induced reoxygenation, in causing HIF-1 activation and vascular radioresistance.

Reoxygenation enhances translation of downstream HIF-1 signals

There is a second, free radical-independent mechanism through which reoxygenation stimulates HIF-1 signaling. Detailed studies of HIF-1 reporter constructs have revealed that exposing hypoxia-cultured cells to a period of reoxygenation enhances downstream HIF-1 signaling (Vordermark et al., 2001). We hypothesized that this phenomenon might account, in part, for the increased expression of HIF-1-regulated genes following radiation in vivo.

First, we optimized the experimental conditions to best examine the effects of hypoxia and reoxygenation on HIF-1 signaling in vitro. In our hands, HRE-GFP fluorescence intensity remains relatively constant during exposure to hypoxia (0.5% O_2) up to 18 hr—after which point the signal increases significantly over time (Figure 5A). A 12 hr incubation at 0.5% O_2, however,

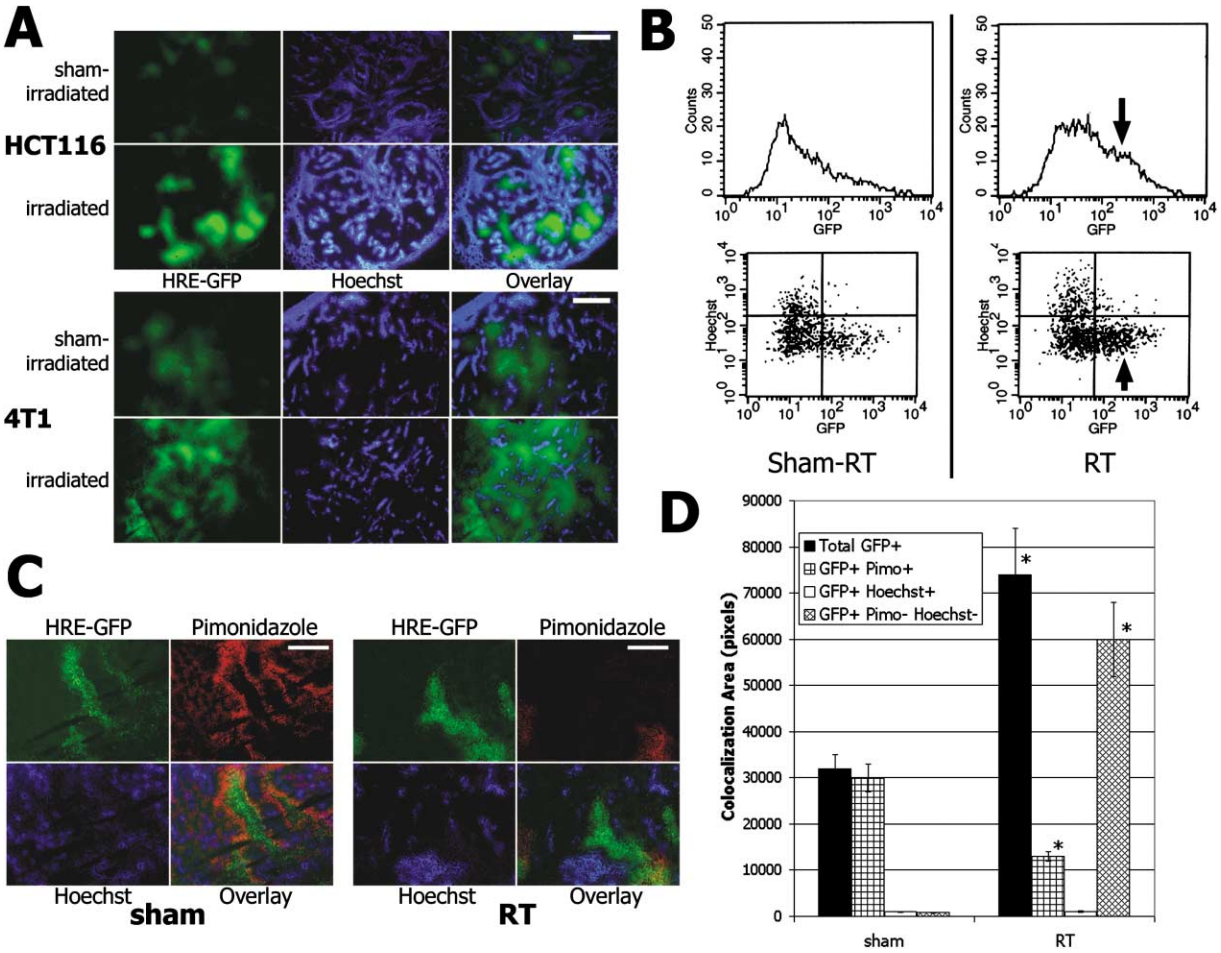

Figure 3. RT-induced HIF-1 activation coincides with reoxygenation

A: Representative tumor sections demonstrating increased GFP intensity in irradiated tumors, but lack of overlap with a perfusion marker (Hoechst) regardless of treatment. Bar = 300 μm.

B: Representative data for HCT116 tumors excised and disrupted to single cells for analysis via flow cytometry. Note increased proportion of GFP-intense counts in irradiated tumors (arrow). Approximately 2% of cells were positive for both GFP and the perfusion marker, regardless of treatment.

C: Representative pimonidazole immunohistochemistry in 4T1 tumors. Pimonidazole staining was closely associated with HRE-GFP expression in sham-treated tumors (see Experimental Procedures). In irradiated tumors, HRE-GFP expression was frequently seen in the absence of hypoxia marker signal. Bar = 50 μm.

D: Quantification of immunohistochemistry staining patterns for 4T1 tumors. HRE-GFP was tightly associated with pimonidazole in nonirradiated tumors. Following irradiation, the majority of the GFP signal was found in pimonidazole-negative tissue. *, $p < 0.05$, versus nonirradiated tumors.

does not appreciably increase HRE-GFP fluorescence intensity in these cells. Therefore, we chose this time point to study, since it would describe the effects of reoxygenation, *specifically*, on HIF-1 signaling. Reoxygenation of hypoxic cells resulted in a complete loss of nuclear HIF-1 within 10 min (data not shown). Despite the lack of nuclear signaling, however, HRE-GFP fluorescence intensity was significantly enhanced during reoxygenation (Figure 5B). In contrast, reoxygenation had no impact on CMV-GFP fluorescence intensity (Figure 5C). Since HIF-1 is not found in the nucleus during reoxygenation, it would be expected that reoxygenation enhancement of HRE-GFP signal occurs independently of mRNA production. Supporting this hypothesis, transcriptional blockade with actinomycin D has no effect on reoxygenation-mediated enhancement HRE-GFP fluorescence intensity. Conversely, inhibiting translation with cycloheximide completely abrogates the response, confirming that active protein production is required for this reoxygenation-mediated enhancement to proceed. Analogous results were seen for the effects of reoxygenation on VEGF secretion in two cell lines (Figure 5D), confirming that these effects are relevant to downstream HIF-1 signaling in general. Of note, cells incubated at 0.5% O_2 for longer periods of time had proportionately similar HRE-GFP signal enhancement after reoxygenation. Reoxygenating cells after exposures of 12, 24, and 48 hr at 0.5% O_2 resulted in increases in fluorescence intensities of 92.86 ± 2.4%, 94.44 ± 1.8%, and 91.78 ± 1.5%, respectively, indicating that this response is relevant to a broad range of potential physiologic exposures to hypoxia.

Together, these results suggest that a protected pool of HIF-1-regulated transcripts are kept untranslated until reoxygenation occurs, at which point robust translation of this mRNA takes place. Thus, we next investigated whether such a hypoxia-inducible translational silencing mechanism might account for the observed effects of radiation and reoxygenation on HIF-1

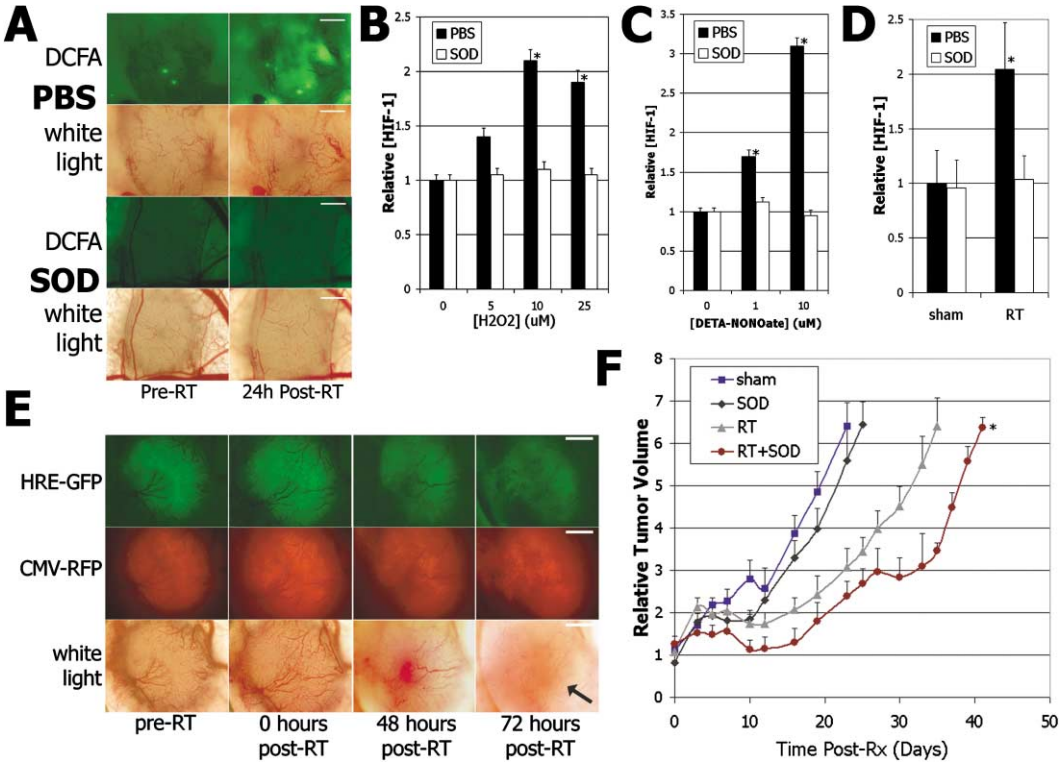

Figure 4. Reoxygenation-induced free radical species upregulate HIF-1

A: Representative microscopy images captured following incubation of window chamber tumors with an ROS-sensitive dye (DCFA). ROS abundance increased during reoxygenation, but was inhibited by treatment with the SOD mimetic. Bar = 300 μm.

B: In vitro, exposing 4T1 cells to H_2O_2 every 20 min for 10 hr resulted in increased nuclear HIF-1 levels, as determined by ELISA. Response was blocked with equimolar amounts of an SOD mimetic. Results were normalized to the sham-treated mean value. *, $p < 0.05$, versus no H_2O_2.

C: In vitro, incubating 4T1 cells with the nitric oxide donor DETA-NONOate (AG Scientific) for 10 hr significantly increased nuclear HIF-1 levels. Coincubation with equimolar concentrations of an SOD mimetic inhibited this response. Results were normalized to the sham-treated mean value. *, $p < 0.05$, versus no nitric oxide donor.

D: Flank tumors randomized to RT (15 Gy) or sham-RT, followed by PBS or SOD mimetic, and excised 48 hr after treatment. Nuclear HIF-1 levels were assayed via ELISA, and results were normalized to the sham-treated mean value. *, $p < 0.05$, RT-SOD versus RT-PBS.

E: HRE-GFP reporter tumors grown in window chambers and randomized to RT (15 Gy) or sham-RT, followed by PBS or SOD mimetic, and monitored using intravital microscopy. Note that GFP fluorescence intensity decreased at 48 hr post-RT (compare to Figure 1B), and that striking vascular destruction occurred by 72 hr after treatment (arrow).

F: Flank tumors randomized to RT or sham-RT, followed by PBS or SOD mimetic, and followed with caliper measurements. *, $p < 0.05$ RT-SOD versus RT-PBS by log-rank analysis.

signaling. A stress-induced translational control mechanism—regulated by so-called stress granules—closely fits our hypoxia-reoxygenation HIF-1 data. Stress granules are cytosolic polymers consisting of nearly half a cell's mRNA bound to distinct RNA shuttling proteins. These granules form in response to a variety of stressors and tightly regulate translation, allowing only the most crucial proteins to be synthesized. Once the stress is alleviated, the granules depolymerize and the surviving cell can then recommence translation and recover appropriately (Anderson and Kedersha, 2002; Kedersha and Anderson, 2002). Although stress granule polymerization had not before been described in response to hypoxia, our data strongly suggested that they might be involved. Therefore, we stained hypoxia-treated cells for a stress granule constituent, TIAR. This staining revealed that stress granules formed in tumor cells following hypoxic incubation after as little as 4 hr. Upon reoxygenation, the granules were no longer detectable (Figure 5E).

We next investigated whether stress granules specifically inhibit the translation of HIF-1-regulated transcripts. We obtained a dominant negative mutant of TIA-1, a key stress granule scaffolding protein (generous gift of Dr. N. Kedersha). This mutant, TIA-1ΔRRM, lacks the RNA recognition motif of the native protein and renders a cell incapable of forming stress granules (Kedersha et al., 1999). By transiently transfecting cells with this mutant, we were able to inhibit stress granule polymerization in response to hypoxia (data not shown). Therefore, we investigated whether inhibiting stress granule activity would alter HIF-1 regulation during hypoxia and reoxygenation. 4T1 cells were transiently transfected with TIA-1 or TIA-1ΔRRM. Cells were then exposed to normoxia (21% O_2, 24 hr), hypoxia (21% O_2,12 hr; 0.5% O_2, 12 hr), or reoxygenation (0.5% O_2, 12 hr; 21% O_2, 12 hr), and HIF-1 signaling was quantified by measuring HRE-GFP intensity. Blocking stress granule formation with TIA-1ΔRRM inhibited the usual hypoxia-mediated translational silencing, resulting in efficient expression of HIF-1-regulated proteins during hypoxic stress (Figure 5F). With nonfunctional stress granules, HIF-1-regulated transcripts were robustly translated during hypoxia, and reoxygenation failed to further upregu-

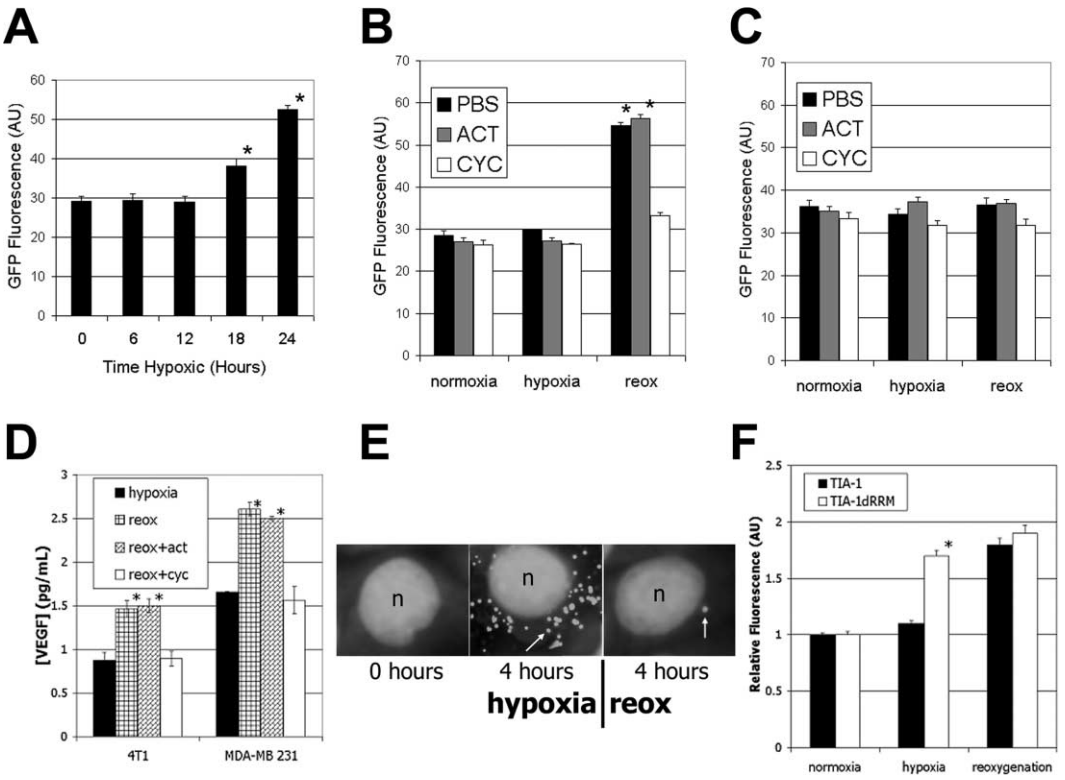

Figure 5. Stress granules suppress downstream HIF-1 signaling

A: 4T1 cells expressing HIF-1-inducible GFP were exposed to 0.5% O_2 for various lengths of time, and the GFP fluorescence intensity was quantified by flow cytometry. *, $p < 0.05$ versus normoxic control.

B: 4T1 cells expressing HRE-GFP were exposed to 24 hr of normoxia (normoxia), 12 hr of normoxia followed by 12 hr of hypoxia (hypoxia), or 12 hr of hypoxia followed by 12 hr of normoxia (reox). During the last 12 hr of the experiment, cells were exposed to PBS, cycloheximide (1 μg/ml), or actinomycin D (1 μg/ml). HRE-GFP fluorescence intensity was quantified by flow cytometry. Reoxygenation induced a translation-dependent, transcription-independent upregulation in downstream HIF-1 activity, as quantified by flow cytometry. *, $p < 0.05$ versus normoxic control.

C: 4T1 cells expressing CMV-GFP were treated and analyzed as in **B**. Reoxygenation had no impact on the fluorescence intensity of these cells.

D: 4T1 and MDA-MB231 cells were treated as in **B**. VEGF secretion into the media increased in a translation-dependent, transcription-independent fashion following reoxygenation, as quantified by ELISA. *, $p < 0.05$ versus hypoxic control.

E: 4T1 cells were exposed to hypoxia (0.5% O_2) with or without reoxygenation (21% O_2), followed by staining for TIAR, a stress granule component. Note the appearance of discrete cytoplasmic granules after a four-hour hypoxic incubation, dissipating rapidly upon reoxygenation (arrows).

F: 4T1 cells expressing HRE-GFP were transfected TIA-1 or with a dominant-negative TIA-1 mutant (TIA-1ΔRRM) and exposed to normoxia, hypoxia, or reoxygenation. A significant increase in the HRE-GFP reporter signal was seen during *hypoxia* in TIA-1ΔRRM-transfected cells, but during *reoxygenation* in cells transfected with the wild-type TIA-1. Data are normalized to the fluorescence intensity of normoxia-incubated cells. *, $p < 0.05$ versus wild-type control.

late HIF-1 signaling. In contrast, cells transfected with wild-type TIA-1 displayed the typical pattern of inefficient downstream HIF-1 signaling after 12 hr of hypoxia, augmented upon reoxygenation. Transfecting the vector control resulted in data similar to that seen upon transfection of wild-type TIA-1 (data not shown). In summary, these data strongly support the conclusion that reoxygenation enhances downstream HIF-1 signaling by depolymerizing stress granules, leading to increased translation of HIF-1-regulated transcripts.

Finally, we sought to determine whether the same patterns of stress granule formation and depolymerization in response to hypoxia and reoxygenation, respectively, could be found in vivo. TIAR staining of sham-irradiated tumor sections revealed that stress granules form in the ambient—hypoxic—tumor environment, and that they colocalize with areas of hypoxic gene activity (Figures 6A and 6B). In line with their proposed importance in radiation-induced HIF-1α signaling, stress granules stain much less intensely in irradiated tumors, suggesting that radiation/reoxygenation leads to their depolymerization. These data support the conclusion that stress granules are involved in regulating hypoxic gene translation in vivo, and that their translational inhibition may be reversed by radiation/reoxygenation.

HIF-1 regulates radiation-induced EC radioresistance

We next sought to determine to what degree postradiation HIF-1 activation regulates vascular radioresistance. As shown above, radiation upregulates the expression of two important cytokines partially regulated by HIF-1—VEGF and bFGF. It would be informative to know whether radiation-induced secretion of these factors is regulated by HIF-1 or by a competing mechanism. If regulated by HIF-1, their expression would be seen in the same pattern as radiation-induced HIF-1 upregulation; i.e., complementary to vascular perfusion. If regulated by an alternative mechanism—for instance, directly induced by radiation through MAPK signaling (Park et al., 2001)—the pattern would likely be much different (i.e., diffuse upregulation throughout the tumor).

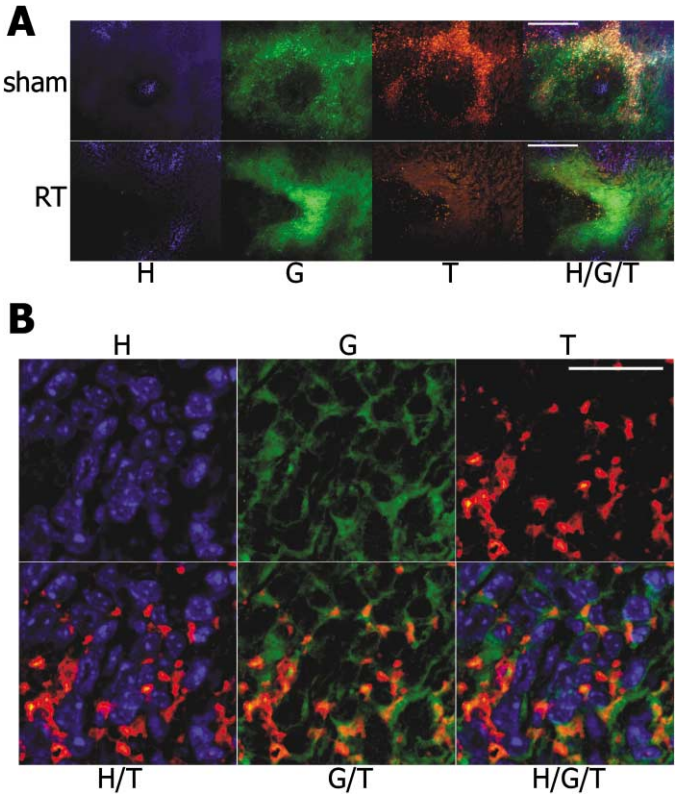

Figure 6. Radiation/reoxygenation destabilizes stress granules in vivo

A: 4T1 HRE-GFP-expressing tumors were irradiated, excised 48 hr later, and stained for TIAR, a stress granule protein. Representative tri-colored sections are shown from irradiated and sham-irradiated tumors, demonstrating typical Hoechst perfusion staining (H), endogenous GFP expression (G), and TIAR staining (T). For nontreated tumors, TIAR staining is most intense in areas of high HIF-1 activity. In post-RT tumors, TIAR staining is weak, although some association with HIF-1 activity is retained. Bar = 50 μm.

B: Sections were prepared as in **A**, followed by brief nuclear counterstaining with Hoechst and imaging at high magnification (100×). Representative tricolored sections are shown from a sham-irradiated tumor. Hoechst stain (H) marks cellular nuclei, and GFP signal (G) marks the cytoplasm. TIAR stain (T) appears granular and completely localized to the cytoplasm. Bar = 10 μm.

To address this issue, irradiated tumors were stained for VEGF and FGF to determine whether a particular staining pattern prevailed. As shown in Figure 7A, postradiation VEGF and bFGF expression overlapped completely with HIF-1 reporter activity. In fact, no staining for either cytokine was ever observed in the absence of HRE-GFP expression in irradiated tumors. This finding strongly implicates radiation-induced HIF-1 upregulation in promoting post-RT VEGF and bFGF secretion. Since they play a strong role in determining the level of EC radiosensitivity, these data support the importance of HIF-1 in regulating radioresistance of the tumor vasculature.

To further explore this hypothesis, siRNA was used to deplete tumor cells of nuclear HIF-1 by knocking down HIF-1α or HIF-1β (Figures 7B). These cells were then exposed to normoxia, radiation, hypoxia, or hypoxia followed by reoxygenation, and the resulting conditioned media was collected to test for radioprotective capacity. The conditioned media was added to irradiated endothelial cells in culture, and EC viability was determined with an MTT assay 72 hr later. Media taken from HIF-1-competent tumor cells exhibited equal EC-radioprotective effects when the tumor cells had been exposed to normoxia, radiation, and hypoxia, but was more potently radioprotective when taken from cells exposed to hypoxia/reoxygenation. In contrast, the conditioned media displayed no significant EC-radioprotective capacity in response to hypoxia/reoxygenation when taken from HIF-1 incompetent cells (Figure 7C). These results suggest that hypoxia/reoxygenation induces tumor cells to secrete EC-radioprotective cytokines through a HIF-1-dependent pathway.

The data presented above support the hypothesis that radiation-induced HIF-1 activation is a vital determinant of vascular radiosensitivity. We sought direct evidence for this hypothesis by investigating the effects of combining radiotherapy with a HIF-1-targeting drug, YC-1 (Yeo et al., 2003). We chose a relatively low YC-1 dose (5 mg/kg), which was found to decrease tumor HIF-1 levels, but to have minimal effects on tumor vascularity or growth rate, alone (data not shown). Also, a relatively low radiation dose (10 Gy) was chosen, which has historically had mild effects on the growth of this tumor model (Lohr et al., 2000). Administered after radiation, this dose of YC-1 caused significant ($p < 0.01$) tumor growth delay, essentially inhibiting tumor regrowth until the drug was discontinued (Figure 8A). Window chamber studies demonstrated that the combination of radiation with YC-1 blocked postradiation HIF-1 upregulation, and resulted in significant vascular destruction (Figure 8B). It was also noted that this combination of therapeutics was selectively toxic for tumor vasculature. Nearby nontumor vessels did not appear to be affected by this treatment, suggesting that combining HIF-1 blockade with radiation may increase antitumor efficacy without enhancing normal tissue damage.

Discussion

Intense research interest has stemmed from the discovery that radiation prompts tumors to promote radioresistance in their vessels, and there is interest in blocking this response to improve treatment efficacy. There are two attractive approaches for developing strategies to target RT-induced EC radioprotection. One option would be to identify in ECs the radioprotective signals initiated by the binding of relevant cytokines. If a common pathway were discovered, blocking this signaling in ECs could then silence the radioprotective message, rendering tumor vessels more sensitive to radiation. Some previously published work has made progress toward this goal, identifying conserved EC signaling pathways, including Raf-1 and PI3K/Akt, used by important radioprotective factors such as VEGF and bFGF (Alavi et al., 2003; Edwards et al., 2002). Though this strategy has shown potential, it has important drawbacks. Specifically, inhibiting EC survival signals would likely have an equal radiosensitizing effect on normal and malignant tissue. Therefore, to achieve a therapeutic advantage, sophisticated mechanisms would be essential to deliver the therapy selectively to tumor vasculature (Hood et al., 2002).

A potentially more promising strategy may be to target the radiation-induced radioprotective response at its source: the tumor cell. Theoretically, if one were able to identify and block a step sufficiently upstream in this pathway, the EC radioprotective response could be inhibited before the protective cytokines were ever released. Not only would this approach achieve efficient vascular radiosensitization, it would be specific for tumor

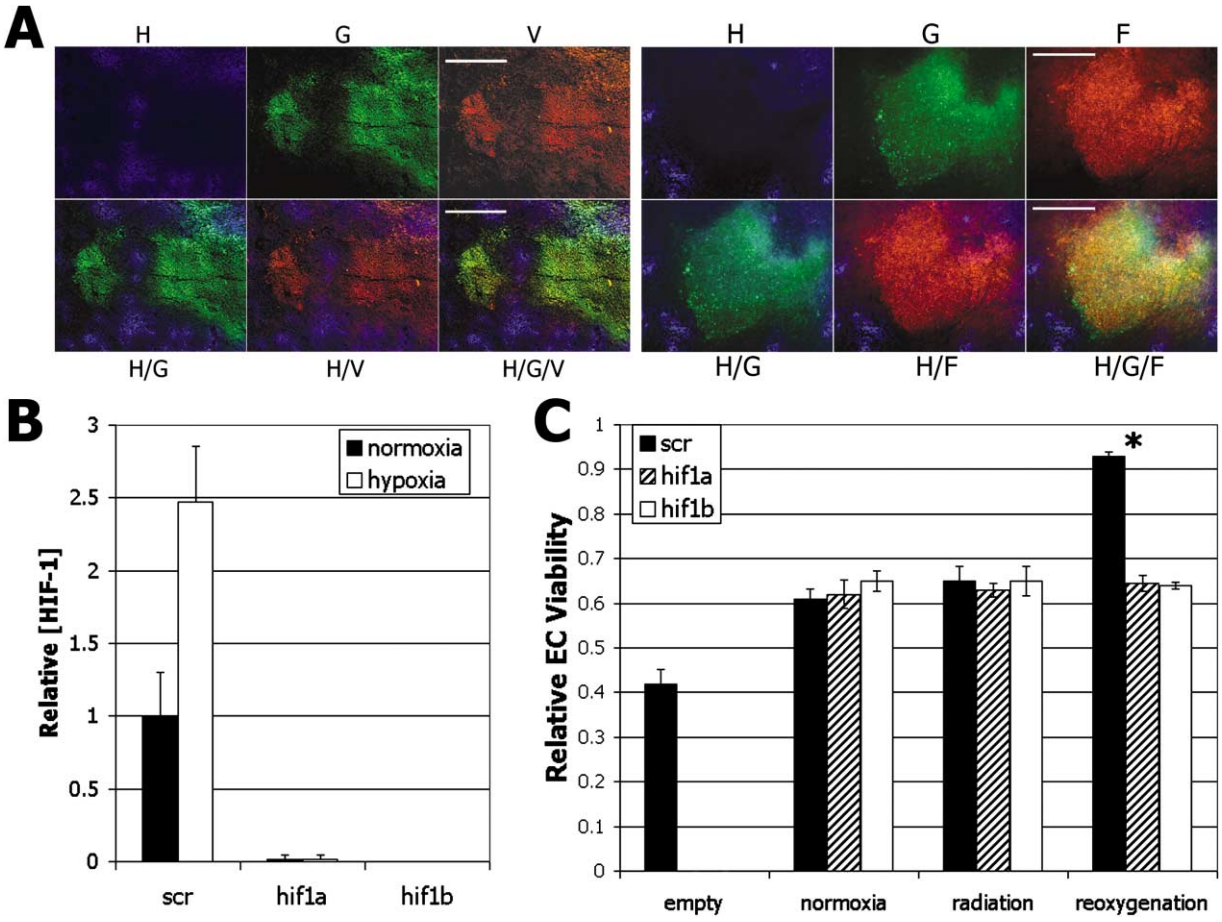

Figure 7. HIF-1 RT response regulates EC radiosensitivity

A: 4T1 HRE-GFP-expressing tumors were irradiated, excised 48 hr later, and stained for VEGF. A representative section showing Hoechst perfusion staining (H), endogenous GFP (G), and VEGF staining (V), as well as overlay images for each. A similar section is shown stained for bFGF (F). Bar = 50 μm.

B: Nuclear HIF-1 levels for 4T1 cells constitutively expressing scrambled (scr), HIF-1α-targeted (hif1a), or HIF-1β-targeted (hif1b) siRNA. Cells were cultured for 12 hr under hypoxic (0.5% O_2) or normoxic (21% O_2) conditions. Both siRNA species virtually eliminate all nuclear HIF-1 accumulation. Results are normalized to the mean HIF-1 level from the normoxia-cultured scrambled cells.

C: Conditioned media from siRNA-expressing 4T1 cells exposed to normoxia, radiation, or reoxygenation was added to irradiated ECs to test for radioprotective capacity (see Experimental Procedures). Nonconditioned media—"empty"—was used as a negative control. Reoxygenation of control tumor cells conferred significant EC-radioprotective capacity on conditioned media, but this effect was lost when the media was conditioned by HIF-1-depleted tumor cells. Results are expressed as the ratio of the MTT OD_{540} for irradiated over nonirradiated ECs. *, $p < 0.05$ scr versus hif1a or hif1b cells.

vessels as well. For these reasons, there appears to be much promise in studying how radiation induces an EC-radioprotective response in tumors for the purpose of developing novel vascular radiosensitizers.

The work presented here takes a significant step toward this goal. We were able to successfully identify a pathway which appears to play a dominant role in regulating the tumor EC-radioprotective response. A dual mechanism, initiated by radiation-induced tumor reoxygenation, leads to significant upregulation of tumor HIF-1 activity. The importance of this response was illustrated in several ways. First, it was shown that after RT, EC-radioprotective cytokines were secreted exclusively in concert with high HIF-1 activity. This is a subtle yet important point. The fact that post-RT VEGF and bFGF expression colocalized so strongly with HIF-1 activation weakens the case for competing mechanisms regulating radiation-induced EC-radioprotection in tumors. This was a somewhat surprising finding, especially in light of data from our studies and others (Gorski et al., 1999; Park et al., 2001) which have demonstrated that radiation can directly cause VEGF secretion from tumor cells in vitro. The discrepancy forces us to consider the possibility that irradiation of cultured cells stimulates VEGF secretion through an "artificial" mechanism, irrelevant to the actual biology found in irradiated tumors, in vivo. It could be speculated that irradiation of cultured cells might cause accumulation of cytokines in the overlying media which do not accumulate in tumor tissue (due to degradation, transport, etc.), and that these cytokines might initiate an autocrine loop culminating in VEGF secretion. This might explain why evidence was lacking for post-RT VEGF and bFGF expression in well-perfused, well-oxygenated tumor tissue. In either case, these immunohistochemistry data strongly support the conclusion that HIF-1 is a major regulator of important known EC-radioprotective cytokines.

Second, we demonstrated that HIF-1-regulated cytokines

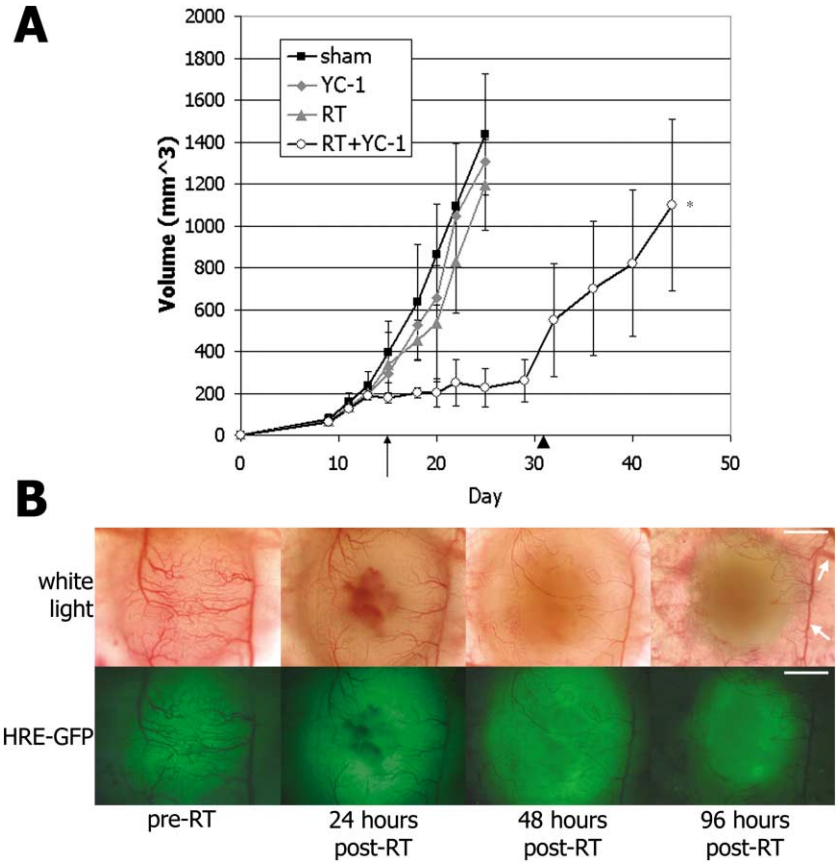

Figure 8. HIF-1 blockade enhances RT efficacy

A: Combining RT with a HIF-1-targeting therapeutic significantly improved tumor growth delay over that with either treatment alone. RT began on day 12, and daily YC-1 injections began on day 15 (arrow). After two weeks without progression, YC-1 was withdrawn to determine whether regrowth would occur (arrowhead). *, $p < 0.05$ versus RT alone by log-rank analysis.

B: Combined radiation and YC-1 treatment resulted in substantial destruction of the tumor vasculature. Post-RT HIF-1 upregulation was inhibited by YC-1 treatment. Regression of tumor vessels was seen as early as 24 hr after RT, and was prominent by 48 hr post-RT (compare to Figure 1B). Arrows highlight the apparent relative resistance of nontumor vessels in the nearby irradiated normal tissue.

are capable of decreasing EC radiosensitivity. Stimulating tumor cells to secrete HIF-1-regulated cytokines confers an EC-radioprotective capacity on tumor-conditioned media. Unexpectedly, depleting cells of HIF-1 activity through knocking down HIF-1α or HIF-1β completely inhibited their ability to mobilize EC radioprotectors in response to hypoxia/reoxygenation. Since hypoxia/reoxygenation seems to be the main stimulus for the radioprotective response in vivo, these results would suggest that HIF-1 plays a dominant role in regulating the radiosensitivity of tumor vasculature following RT.

The importance of HIF-1's dominance here was verified by demonstrating significantly improved tumor control when irradiation was combined with a HIF-1 inhibitor. YC-1, which was capable of suppressing HIF-1 activity at low doses (5 mg/kg) in our hands, was potently synergistic in this study. It had dramatic vascular destabilizing effects on the tumor vasculature without any visible impact on the surrounding normal vessels. These data support the conclusion that post-RT HIF-1 may be a major determinant of tumor radiosensitivity.

Our results also raise some interesting questions about how endothelial cells respond to radiation. Although apoptosis is commonly induced by RT, it may not be the dominant mechanism of radiation-induced death for many cell types (Abend, 2003). Some data supports the hypothesis that apoptosis is the main mechanism whereby endothelial cells die in response to radiation damage (Garcia-Barros et al., 2003; Paris et al., 2001). However, it is difficult to reconcile these findings with some other strong evidence in the literature. For example, though EC apoptosis peaks 4–8 hr following RT, radiation-induced vascular destruction typically begins 48 hr later (Geng et al., 2001). Moreover, the percentage of ECs undergoing apoptosis following clinical doses of RT is usually between 0 and 8% (Edwards et al., 2002; Garcia-Barros et al., 2003)—a change which may or may not be able to account for the vascular damage typically seen with these doses. Along the same lines, it seems illogical that HIF-1 activation (occurring 40 hr after peak EC apoptosis) would have an effect on the vasculature; that is, unless apoptosis is not the sole significant mechanism of EC death in response to RT. Intriguingly, work by others has shown that combining RT with angiostatin causes significantly enhanced EC cytotoxicity without an accompanying increase in the levels of EC apoptosis (Mauceri et al., 1998). These studies, along with the data presented above, support the concept that endothelial cells may undergo significant nonapoptotic cell death in response to radiation, and that the release of cytokines by tumor cells can suppress these effects.

The biology unveiled here by our model aptly demonstrates an important emerging concept in HIF-1 signaling: that hypoxia is only a piece of the puzzle. Upon discovering that radiation led to reoxygenation-associated HIF-1 upregulation, we sought to determine which of the potential intermediating mechanisms accounted for this finding. We considered that post-RT HIF-1 upregulation might be due to radiation, reoxygenation, or reoxygenation-induced free radical formation. Followup in vitro studies supported only the latter two hypotheses. Thus, we sought to document and understand how oxidative stress and reoxygenation both lead to increased activity of the HIF-1 pathway.

Recent work has shown that diverse free radical species have potent stabilizing effects on HIF-1 in vitro (Brune et al., 2003; Chandel et al., 1998, 2000; Gao et al., 2002; Haddad and Land, 2001; Park et al., 2003; Zhou et al., 2003). However, there is still a large amount of conflicting data on the topic. Especially controversial has been the role of nitric oxide in regulating HIF-1. Some early work suggested that nitric oxide exerts inhibitory effects on HIF-1 (Adhikary et al., 2000; Huang et al., 1999), but several other studies have shown the opposite to be true (Kasuno et al., 2003; Metzen et al., 2003; Sandau et al., 2001). Recent elegant studies have somewhat clarified these discrepancies. (Mateo et al., 2003; Wellman et al., 2003), It has been shown that low (physiologic) NO concentrations may block unnecessary HIF-1 activation, but high (pathologic) concentrations facilitate its activation (Mateo et al., 2003). Also, the effects of NO on HIF-1 stability appear to be context-dependent, influenced by the presence or absence of key accessory oxidative species (Wellman et al., 2003). Our studies contribute to the debate over oxidative stress and HIF-1 by demonstrating that: (1) free radical species cause tumor HIF-1 activation in vivo, and (2) free radical species are abundant in clinically relevant tumor treatment models. Since the free radical marker and scavenger used here are both highly species-insensitive, little can be learned from this study about *which* oxidative species might regulate HIF-1 in vivo. Even so, this study takes a significant first step toward validating that free radical species are important signaling molecules in tumors, and that they act—in certain scenarios, at least—to increase HIF-1 activity. These data highlight the importance of continuing in vivo investigation of the role of tumor free radicals in HIF-1 regulation.

This work adds yet another layer to the complexity of HIF-1 signaling—posttranscriptional silencing of HIF-1-regulated genes. Historically, three regulatory points have been recognized where HIF-1 activity might be modulated: transcription rate, protein degradation rate, and nuclear activity (Semenza, 2002). The data presented here make it clear, though, that HIF-1 nuclear signaling is not the final determinant of activity in the HIF-1 pathway. During hypoxia, HIF-1-regulated transcripts are partially sequestered in stress granules, resulting in a downregulation of HIF-1 signaling. Upon reoxygenation, the cell is able to rapidly translate the once-sequestered HIF-1-regulated transcripts, allowing it to recover from the hypoxic shock and prepare for future insults. This is a compelling finding, as it suggests that stress granules may cause hypoxia-regulated genes to be most efficiently translated *after* a hypoxic exposure. What is unknown is to what degree HIF-1-regulated transcripts might be preferentially included or excluded from stress granules during hypoxia. It has been observed that certain transcripts are selectively excluded from stress granules during exposure to specific stressors (Collier et al., 1988; Nover et al., 1989). It would be interesting to know, then, which of HIF-1's target gene mRNAs are efficiently translated during hypoxia and which require reoxygenation for full activity. This question also merits further investigation.

Experimental procedures

Reporter construct

A HIF-1-inducible fluorescent reporter construct was created by splicing five copies of the hypoxia regulatory element (HRE) upstream of enhanced green fluorescent protein (GFP). Along with this construct, a constitutive RFP expression vector was transduced into target cells to serve as an internal fluorescence control. For details, see the Supplemental Data at http://www.cancercell.org/cgi/content/full/5/5/429/DC1.

Tumor models

Window chamber implantation was carried out on 8- to 10-week-old mice as described previously (Dewhirst et al., 1990). For details, see the Supplemental Data. Unless stated otherwise, all in vivo experiments were performed with 5 mice per group.

Tumor treatments

Mice fit with window chambers were randomized to treatment groups once tumors reached 3 mm in diameter; mice with fat pad or flank tumors were randomized once tumors were 1 cm in diameter. All radiation was delivered in 5 Gy fractions, with 24 hr intervals separating doses in fractionated treatment, using a Mark IV cesium irradiator (dose rate = 7 Gy/min, JL Shepherd, San Fernando, CA). Unless otherwise noted, radiation was delivered to a total dose of 15 Gy. As indicated in the text, in some instances, an SOD mimetic (AEOL-10113) or HIF-1α inhibitor (YC-1) were combined with radiation. These drugs were administered following RT to avoid interfering with the radiation dose. SOD mimetic treatments (10 mg/kg, IP) were administered every 24 hr for three days (0 hr, 24 hr, 48 hr). YC-1 treatments (5 mg/kg, IP) were administered every 24 hr for the times indicated.

In vivo microscopy

Observations of window chamber tumors were performed daily on restrained, unanesthetized mice using an inverted Zeiss fluorescence microscope, and images were analyzed using Adobe Photoshop (for details, see Supplemental Data).

Immunohistochemistry

A hypoxia marker, pimonidazole (70 mg/kg, IP; Chemicon), and a perfusion marker, Hoechst 33342 (1 mg/mouse, IV; Sigma), were administered 3 hr and 30 min prior to tumor excision, respectively. Subsequent immunofluorescence was performed on frozen sections of these excised tumors (for details, see Supplemental Data).

Flow cytometry

Hoechst 33342 (1 mg/mouse, IV; Sigma) was delivered thirty minutes prior to removing flank and mammary tumors. Excised tumors were processed to single cell suspensions and analyzed for Hoechst and GFP using flow cytometry (for details, see Supplemental Data).

Protein quantification

Tumor homogenates and tissue culture samples were both used for protein analysis. All samples were processed using a Nuclear Extraction Kit (ActiveMotif), and all were normalized by total protein content using a Bradford-based assay (Promega). Nuclear extract HIF-1 levels were quantified with a HIF-1 ELISA kit (ActiveMotif). Crude extract VEGF levels were also assayed using an ELISA kit (R&D Systems). PAI-1 and FGF levels were determined semiquantitatively by Western blot, using a polyclonal goat anti-PAI-1 antibody (SantaCruz, #sc-6642) and a polyclonal rabbit anti-FGF antibody (SantaCruz, #sc-79), detected with HRP-conjugated donkey anti-goat or donkey anti-rabbit secondary antibodies (SantaCruz).

In vivo ROS analysis

Wild-type 4T1 tumors were grown in window chambers and exposed to an ROS-sensitive dye (carboxy-2′7′-dihydrodichlorofluorescein diacetate, H_2DCFDA, Molecular Probes) or an ROS-insensitive dye (carboxy-2′7′-dichlorofluorescein diacetate, DCFDA, Molecular Probes). Mice were anesthetized, and the dye (10 μM) was suffused over tumor tissue for 30 min. After washing with saline, the cover glass was replaced, and the dichlorofluorescein signal was detected using intravital microscopy, as described above.

Stress granule assays

For visualization of stress granules, cells were plated on poly-L-lysine-treated coverslips, exposed to hypoxia (0.5% oxygen), and stained with a goat polyclonal anti-TIAR antibody (SantaCruz). To inhibit stress granule formation, 4T1 cells stably transfected with the HIF-1α reporter were transiently cotransfected with TIA-1/CMV-RFP, or TIA-1ΔRRM/CMV-RFP at a 10-to-1

ratio using Lipofectamine 2000 (Invitrogen). After a 24 hr recovery period, the cells were incubated under normoxic or hypoxic conditions for the times indicated, and analyzed using flow cytometry. Positive transfectants were identified by RFP fluorescence intensity greater than 99% over that of non-transfected controls. Cells were then analyzed for GFP intensity to determine HIF-1α reporter activity.

siRNA constructs

A retroviral siRNA expression vector (pSuper.retro, Oligoengine) was used to stably introduce the following target siRNA sequences to 4T1 cells: AGAG GTGGATATGTCTGGG (HIF-1α), AATGACATCAGATGTACCA (HIF-1β), GGGTCTGTATAGGTGGAGA (scramble). Transductants were selected with puromycin (2 μg/ml).

EC viability assay

6-well plates were seeded with 10^5 siRNA-expressing 4T1 cells covered with growth media. 12 hr later, the plates were randomized to: (1) 24 hr normoxia, (2) 10 Gy radiation, followed by 24 hr normoxia, (3) 12 hr hypoxia followed by 12 hr normoxia, or (4) 12 hr normoxia followed by 12 hr hypoxia. Simultaneously, 96-well plates were seeded with 10^3 SVEC cells in growth media. 24 hr later, the ECs were irradiated (10 Gy), and the growth media was immediately replaced with either tumor-conditioned media or fresh growth media. 72 hr later, 1 mg/ml MTT (Sigma) was added to the EC media. 4 hr later, the MTT crystals were dissolved in DMSO, and read on a spectrophotometer at OD_{540}.

Statistics

Unless otherwise noted, data are reported as a mean $\pm$ standard deviations. Statistical significance was determined using a Student's t test or ANOVA, where appropriate, and p values less than 0.05 were considered significant.

Acknowledgments

We would like to thank I. Batinic-Haberle for providing AEOL-10113 and N. Kedersha for providing TIA-1ΔRRM, Z. Rabbani for providing technical assistance, and P. Kelly, J. Trani, and D. McDonnell for providing their advice and suggestions. Support was provided by funds from the Duke SPORE in breast cancer, NIH/NCI 40355, and the Howard Hughes Medical Institute.

Received: December 10, 2003
Revised: February 25, 2004
Accepted: March 15, 2004
Published: May 17, 2004

References

Abend, M. (2003). Reasons to reconsider the significance of apoptosis for cancer therapy. Int. J. Radiat. Biol. *79*, 927–941.

Adhikary, G., Premkumar, D.R., and Prabhakar, N.R. (2000). Dual influence of nitric oxide on gene regulation during hypoxia. Adv. Exp. Med. Biol. *475*, 285–292.

Alavi, A., Hood, J.D., Frausto, R., Stupack, D.G., and Cheresh, D.A. (2003). Role of Raf in vascular protection from distinct apoptotic stimuli. Science *301*, 94–96.

Anderson, P., and Kedersha, N. (2002). Visibly stressed: The role of eIF2, TIA-1, and stress granules in protein translation. Cell Stress Chaperones *7*, 213–221.

Batinic-Haberle, I., Benov, L., Spasojevic, I., and Fridovich, I. (1998). The ortho effect makes manganese(III) meso-tetrakis(N-methylpyridinium-2-yl) porphyrin a powerful and potentially useful superoxide dismutase mimic. J. Biol. Chem. *273*, 24521–24528.

Brune, B., Zhou, J., and von Knethen, A. (2003). Nitric oxide, oxidative stress, and apoptosis. Kidney Int. Suppl. *84*, S22–S24.

Bussink, J., Kaanders, J.H., Rijken, P.F., Raleigh, J.A., and Van der Kogel, A.J. (2000). Changes in blood perfusion and hypoxia after irradiation of a human squamous cell carcinoma xenograft tumor line. Radiat. Res. *153*, 398–404.

Camphausen, K., and Menard, C. (2002). Angiogenesis inhibitors and radiotherapy of primary tumours. Expert Opin. Biol. Ther. *2*, 477–481.

Carlevaro, M.F., Albini, A., Ribatti, D., Gentili, C., Benelli, R., Cermelli, S., Cancedda, R., and Cancedda, F.D. (1997). Transferrin promotes endothelial cell migration and invasion: implication in cartilage neovascularization. J. Cell Biol. *136*, 1375–1384.

Chandel, N.S., Maltepe, E., Goldwasser, E., Mathieu, C.E., Simon, M.C., and Schumacker, P.T. (1998). Mitochondrial reactive oxygen species trigger hypoxia-induced transcription. Proc. Natl. Acad. Sci. USA *95*, 11715–11720.

Chandel, N.S., McClintock, D.S., Feliciano, C.E., Wood, T.M., Melendez, J.A., Rodriguez, A.M., and Schumacker, P.T. (2000). Reactive oxygen species generated at mitochondrial complex III stabilize hypoxia-inducible factor-1alpha during hypoxia: A mechanism of O2 sensing. J. Biol. Chem. *275*, 25130–25138.

Collier, N.C., Heuser, J., Levy, M.A., and Schlesinger, M.J. (1988). Ultrastructural and biochemical analysis of the stress granule in chicken embryo fibroblasts. J. Cell Biol. *106*, 1131–1139.

Denekamp, J. (1993). Review article: Angiogenesis, neovascular proliferation and vascular pathophysiology as targets for cancer therapy. Br. J. Radiol. *66*, 181–196.

Devy, L., Blacher, S., Grignet-Debrus, C., Bajou, K., Masson, V., Gerard, R.D., Gils, A., Carmeliet, G., Carmeliet, P., Declerck, P.J., et al. (2002). The pro- or antiangiogenic effect of plasminogen activator inhibitor 1 is dose dependent. FASEB J. *16*, 147–154.

Dewhirst, M.W., Oliver, R., Tso, C.Y., Gustafson, C., Secomb, T., and Gross, J.F. (1990). Heterogeneity in tumor microvascular response to radiation. Int. J. Radiat. Oncol. Biol. Phys. *18*, 559–568.

Edwards, E., Geng, L., Tan, J., Onishko, H., Donnelly, E., and Hallahan, D.E. (2002). Phosphatidylinositol 3-kinase/Akt signaling in the response of vascular endothelium to ionizing radiation. Cancer Res. *62*, 4671–4677.

Fenton, B.M., Paoni, S.F., Koch, C.J., and Lord, E.M. (1998). Effect of local irradiation on tumor oxygenation, perfused vessel density, and development of hypoxia. Adv. Exp. Med. Biol. *454*, 619–628.

Folkman, J. (2002). Role of angiogenesis in tumor growth and metastasis. Semin. Oncol. *29*, 15–18.

Folkman, J., and Shing, Y. (1992). Angiogenesis. J. Biol. Chem. *267*, 10931–10934.

Gao, N., Ding, M., Zheng, J.Z., Zhang, Z., Leonard, S.S., Liu, K.J., Shi, X., and Jiang, B.H. (2002). Vanadate-induced expression of hypoxia-inducible factor 1 alpha and vascular endothelial growth factor through phosphatidylinositol 3-kinase/Akt pathway and reactive oxygen species. J. Biol. Chem. *277*, 31963–31971.

Garcia-Barros, M., Paris, F., Cordon-Cardo, C., Lyden, D., Rafii, S., Haimovitz-Friedman, A., Fuks, Z., and Kolesnick, R. (2003). Tumor response to radiotherapy regulated by endothelial cell apoptosis. Science *300*, 1155–1159.

Geng, L., Donnelly, E., McMahon, G., Lin, P.C., Sierra-Rivera, E., Oshinka, H., and Hallahan, D.E. (2001). Inhibition of vascular endothelial growth factor receptor signaling leads to reversal of tumor resistance to radiotherapy. Cancer Res. *61*, 2413–2419.

Gold, L.I., Jussila, T., Fusenig, N.E., and Stenback, F. (2000). TGF-beta isoforms are differentially expressed in increasing malignant grades of HaCaT keratinocytes, suggesting separate roles in skin carcinogenesis. J. Pathol. *190*, 579–588.

Gorski, D.H., Beckett, M.A., Jaskowiak, N.T., Calvin, D.P., Mauceri, H.J., Salloum, R.M., Seetharam, S., Koons, A., Hari, D.M., Kufe, D.W., et al. (1999). Blockage of the vascular endothelial growth factor stress response increases the antitumor effects of ionizing radiation. Cancer Res. *59*, 3374–3378.

Haddad, J.J., and Land, S.C. (2001). A non-hypoxic, ROS-sensitive pathway mediates TNF-alpha-dependent regulation of HIF-1alpha. FEBS Lett. *505*, 269–274.

Hammond, E.M., Dorie, M.J., and Giaccia, A.J. (2003). ATR/ATM targets are phosphorylated by ATR in response to hypoxia and ATM in response to reoxygenation. J. Biol. Chem. *278*, 12207–12213.

Hess, C., Vuong, V., Hegyi, I., Riesterer, O., Wood, J., Fabbro, D., Glanzmann, C., Bodis, S., and Pruschy, M. (2001). Effect of VEGF receptor inhibitor PTK787/ZK222584 [correction of ZK222548] combined with ionizing radiation on endothelial cells and tumour growth. Br. J. Cancer *85*, 2010–2016.

Hood, J.D., Bednarski, M., Frausto, R., Guccione, S., Reisfeld, R.A., Xiang, R., and Cheresh, D.A. (2002). Tumor regression by targeted gene delivery to the neovasculature. Science *296*, 2404–2407.

Huang, L.E., Willmore, W.G., Gu, J., Goldberg, M.A., and Bunn, H.F. (1999). Inhibition of hypoxia-inducible factor 1 activation by carbon monoxide and nitric oxide. Implications for oxygen sensing and signaling. J. Biol. Chem. *274*, 9038–9044.

Jaquet, K., Krause, K., Tawakol-Khodai, M., Geidel, S., and Kuck, K.H. (2002). Erythropoietin and VEGF exhibit equal angiogenic potential. Microvasc. Res. *64*, 326–333.

Jonca, F., Ortega, N., Gleizes, P.E., Bertrand, N., and Plouet, J. (1997). Cell release of bioactive fibroblast growth factor 2 by exon 6-encoded sequence of vascular endothelial growth factor. J. Biol. Chem. *272*, 24203–24209.

Kallman, R.F. (1972). The phenomenon of reoxygenation and its implications for fractionated radiotherapy. Radiology *105*, 135–142.

Kasuno, K., Takabuchi, S., Fukuda, K., Kizaka-Kondoh, S., Yodoi, J., Adachi, T., Semenza, G.L., and Hirota, K. (2003). Nitric oxide induces hypoxia-inducible factor 1 activation that is dependent on MAP kinase and phosphatidylinositol 3-kinase signaling. J. Biol. Chem. *4*, 2550–2558.

Kedersha, N., and Anderson, P. (2002). Stress granules: Sites of mRNA triage that regulate mRNA stability and translatability. Biochem. Soc. Trans. *30*, 963–969.

Kedersha, N.L., Gupta, M., Li, W., Miller, I., and Anderson, P. (1999). RNA-binding proteins TIA-1 and TIAR link the phosphorylation of eIF-2 alpha to the assembly of mammalian stress granules. J. Cell Biol. *147*, 1431–1442.

Kozin, S.V., Boucher, Y., Hicklin, D.J., Bohlen, P., Jain, R.K., and Suit, H.D. (2001). Vascular endothelial growth factor receptor-2-blocking antibody potentiates radiation-induced long-term control of human tumor xenografts. Cancer Res. *61*, 39–44.

Lohr, F., Hu, K., Haroon, Z., Samulski, T.V., Huang, Q., Beaty, J., Dewhirst, M.W., and Li, C.Y. (2000). Combination treatment of murine tumors by adenovirus-mediated local B7/IL12 immunotherapy and radiotherapy. Mol. Ther. *2*, 195–203.

Lund, E.L., Bastholm, L., and Kristjansen, P.E. (2000). Therapeutic synergy of TNP-470 and ionizing radiation: effects on tumor growth, vessel morphology, and angiogenesis in human glioblastoma multiforme xenografts. Clin. Cancer Res. *6*, 971–978.

Mateo, J., Garcia-Lecea, M., Cadenas, S., Hernandez, C., and Moncada, S. (2003). Regulation of hypoxia-inducible factor-1alpha by nitric oxide through mitochondria-dependent and -independent pathways. Biochem. J. *376*, 537–544.

Mauceri, H.J., Hanna, N.N., Beckett, M.A., Gorski, D.H., Staba, M.J., Stellato, K.A., Bigelow, K., Heimann, R., Gately, S., Dhanabal, M., et al. (1998). Combined effects of angiostatin and ionizing radiation in antitumour therapy. Nature *394*, 287–291.

Metzen, E., Zhou, J., Jelkmann, W., Fandrey, J., and Brune, B. (2003). Nitric oxide impairs normoxic degradation of HIF-1alpha by inhibition of prolyl hydroxylases. Mol. Biol. Cell *14*, 3470–3481.

Ning, S., Laird, D., Cherrington, J.M., and Knox, S.J. (2002). The antiangiogenic agents SU5416 and SU6668 increase the antitumor effects of fractionated irradiation. Radiat. Res. *157*, 45–51.

Nover, L., Scharf, K.D., and Neumann, D. (1989). Cytoplasmic heat shock granules are formed from precursor particles and are associated with a specific set of mRNAs. Mol. Cell. Biol. *9*, 1298–1308.

Paris, F., Fuks, Z., Kang, A., Capodieci, P., Juan, G., Ehleiter, D., Haimovitz-Friedman, A., Cordon-Cardo, C., and Kolesnick, R. (2001). Endothelial apoptosis as the primary lesion initiating intestinal radiation damage in mice. Science *293*, 293–297.

Park, J.S., Qiao, L., Su, Z.Z., Hinman, D., Willoughby, K., McKinstry, R., Yacoub, A., Duigou, G.J., Young, C.S., Grant, S., et al. (2001). Ionizing radiation modulates vascular endothelial growth factor (VEGF) expression through multiple mitogen activated protein kinase dependent pathways. Oncogene *20*, 3266–3280.

Park, J.H., Kim, T.Y., Jong, H.S., Chun, Y.S., Park, J.W., Lee, C.T., Jung, H.C., Kim, N.K., and Bang, Y.J. (2003). Gastric epithelial reactive oxygen species prevent normoxic degradation of hypoxia-inducible factor-1alpha in gastric cancer cells. Clin. Cancer Res. *9*, 433–440.

Sandau, K.B., Fandrey, J., and Brune, B. (2001). Accumulation of HIF-1alpha under the influence of nitric oxide. Blood *97*, 1009–1015.

Semenza, G. (2002). Signal transduction to hypoxia-inducible factor 1. Biochem. Pharmacol. *64*, 993–998.

Vordermark, D., Shibata, T., and Brown, J.M. (2001). Green fluorescent protein is a suitable reporter of tumor hypoxia despite an oxygen requirement for chromophore formation. Neoplasia *3*, 527–534.

Wellman, T.L., Jenkins, J., Penar, P.L., Tranmer, B., Zahr, R., and Lounsbury, K.M. (2003). Nitric oxide and reactive oxygen species exert opposing effects on the stability of hypoxia inducible factor-1alpha (HIF-1alpha) in explants of human pial arteries. FASEB J. *18*, 379–381.

Yeo, E.J., Chun, Y.S., Cho, Y.S., Kim, J., Lee, J.C., Kim, M.S., and Park, J.W. (2003). YC-1: a potential anticancer drug targeting hypoxia-inducible factor 1. J. Natl. Cancer Inst. *95*, 516–525.

Zhou, J., Fandrey, J., Schumann, J., Tiegs, G., and Brune, B. (2003). NO and TNF-alpha released from activated macrophages stabilize HIF-1alpha in resting tubular LLC-PK1 cells. Am. J. Physiol. Cell Physiol. *284*, C439–C446.